International Journal of Advanced and Applied Sciences, 2(12) 2015, Pages: 42-46

Contents lists available at Science-Gate

International Journal of Advanced and Applied Sciences

Journal homepage: http://www.science-gate.com/IJAAS.html

Experimental validation for Comsol model of a DEP device

Yavuz Genc [1], Emre Altınağaç [1], Levent Trabzon[1, 2, *]

[1]Department of Nanoscience & Nanoengineering, Istanbul Technical University, Istanbul, Turkey
[2]Department of Mechanical Engineering, Istanbul Technical University, Istanbul, Turkey

ARTICLE INFO

Article history:
Received 27 December 2015
Received in revised form
20 January 2016
Accepted 20 January 2016

Keywords:
AC di-electrophoresis
Microfluidics
Particle Separation
Lab-on-a-Chip
Comsol simulation of DEP

ABSTRACT

In the near future we will see complicated and sophisticated LoC (Lab-on-a-chip) devices for many kinds of medical application which will fit on ones palm and does the job of a high tech laboratory. We successfully compare comsol model with experimental findings for polystyrene particle separation. The green particles with 9.8 μm diameter were directed to certain outlet under negative di-electrophoresis conditions. Basically this paper will cover the Comsol simulations of di-electrophoresis based LoC devices to separate the micro-particles.

1. Introduction

Microfluidic solutions for particle separation generally consist of design, fabrication and characterization steps and this leads to old style trial-error approach. Micro fabrication methods generally take several days to build a microfluidic device and may be another day to setup the experiment. Taking meaningful results almost took several weeks with the trial error approach.

In this paper dielectrophoresis based particle separation simulations with Comsol is demonstrated. Micro channels, electrodes and particles modeled and then estimation of dielectrophoretic and drag force acting on the particles under the different voltage and flowrates covered. Forces and resulting particle trajectories created the separation results for the given parameters in Comsol model. As a final step validation of the Comsol model done via the experimentation at the same parameters applied in simulation.

2. Theory

The simplest theoretical model for DEP is that of a homogeneous spherical particle immersed in a dielectric medium. In a non-uniform electric field, the homogeneous spherical particle influences by a net dielectrophoretic force (Pethig, 2010). The magnitude of this force depends on the polarizability of the particle with respect to medium as well as physical parameters and electrode setup. If a particle has polarizability higher than the medium, the DEP force will push the particle to regions of higher electric field see Fig. 1a pDEP. If the medium has a higher polarizability than the particle, the particle will go to low field strength see Fig. 1b nDEP.

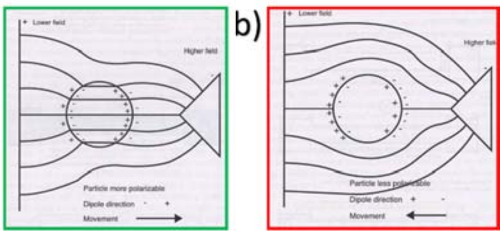

Fig. 1: Spherical particle under non-uniform electric field; a) pDEP, b) nDEP

In microscopic scale DEP force can be written as [X-X];

$$F_{DEP} = \mathrm{Re}\left[\rho(\omega)\nabla E\right] \qquad (1)$$

In the equation E stands for the electric field, ω angular frequency (ω) corresponds to dipole momentum of the particle, which caused by the electric field and Re [...] corresponds to real part of the variables.

This equation becomes as below when its time average obtained:

$$\left\langle \mathrm{F_{DEP}} \right\rangle = 2\pi a^3 \varepsilon_m \,\mathrm{Re}\left[k(\omega)\right]\nabla\left|E_{rms}\right|^2 \qquad (2)$$

∇ gradient of electric field, k(ω) corresponds to Clausius-Mossotti (CM) factor which is stated as [X-X];

$$k(\omega) = \frac{\tilde{\varepsilon}_p - \tilde{\varepsilon}_m}{\tilde{\varepsilon}_p + 2\tilde{\varepsilon}_m} \qquad (3)$$

* Corresponding Author.
Email Address: levent.trabzon@itu.edu.tr

$\tilde{\varepsilon}_p$ and $\tilde{\varepsilon}_m$ are particle and medium dielectric constants. Dielectric constants obtained from the equation of: $\tilde{\varepsilon} = \varepsilon - j\sigma/\omega$ where $j = -1^{\frac{1}{2}}$. In this equation ε shows the dielectric permeability and σ shows the conductivity.

Clausius-Mossotti factor is the measure of the particle and medium relative permittivity (Khoshmanesh et al., 2011). CM factor, depends on the applied electric field frequency, specifies the direction of dielectrophoretic force. According to equation (2) the dielectrical properties and diameter of the particle used for manipulating a particle.
In the continuous flow case the drag force acting on a particle introduced as another force and it's relation with the dielectric force needs to be considered. The equation 1.4 indicated the relationship between the fluid flow and particle movement where "u" is the particle velocity and "v" is the fluid velocity, m_p is the particle mass and τ_p is the particle response time.

$$F_{drag} = \frac{1}{\tau_p} m_p (u - v) \tag{4}$$

The method of Comsol simulation lies on the modelling of the physics under the known parameters and guess the resulting parameters with finite elemenent modelling (Green et al. 2002). DEP device simulation starts with choosing the physical interactions like electrostatic, fluid flow, particle tracing (Altinagac et al., 2014; 2015) and then continuous with the creation of geometry and defining the materials and properties of the materials. Similar to all numerical solution methods boundary conditions, initial conditions assigned before the mesh creation for finite element methods. After that, solver configuration and solution requirements entered to the model like time and error range. Next step is to initiating the solver that creates the results and use the resulting data to create graphs for the reports.

3. Design and simulations

New electrode design - angular interdigitated electrodes- modeled for the continuous polystyrene particle manipulation is drawn as seen in Fig.2. Figure basicly demonstrates the mask designs of the microfluidic channels and electrode configurations. 3.2 µm red fluorescence and 9.8 µm green fluorescence particles supplied from Termoscientific for the model.

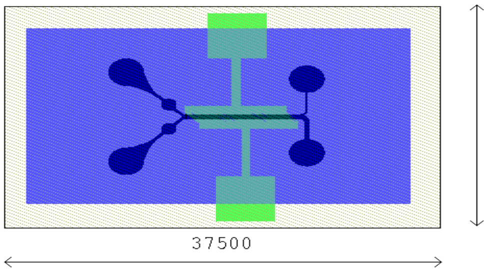

Fig. 2: Mask design of system, the colors indicate: Titanium Electrode, PDMS Micro channel, Glass Substrate (All dimensions are in µ).

In order to demonstrate the design better a 3D CAD model designed and Fig. 3 shows the 3D CAD model of the device. It includes the electrodes, micro channel, electrical connections, inlets and outlets of the channel.

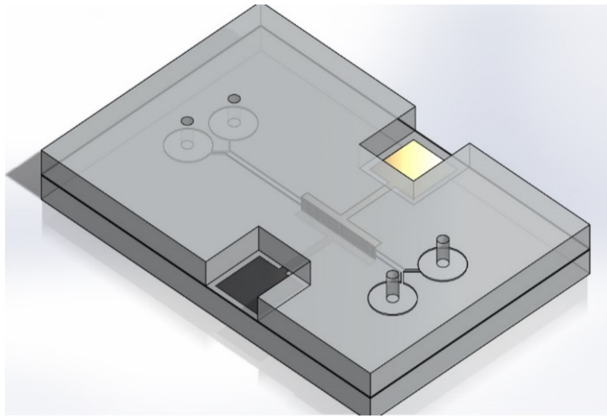

Fig. 3: 3D CAD model of the device

The width of the inlets is the half of the channel width that is 250 µm and they have fillets in the entrance. The outlets are asymmetric, the lower one is 150 µm, and upper one is 350 µm.

Constants and simulation parameters in model are given in Table 1.

Table 1: Model simulation parameters and constants

Constant parameters			
Channel length (µm)	Height (µm)	Channel width (µm)	Electrode width (µm)
10000	12.5	500	50
Relative Permittivity (RP) of DI water	Density of water [kg/m3]	Density of polystyrene particles [kg/m3]	Electrode angle (°)
120	1000	1050	45
RP of polystyrene particles	Voltage (V)	Flowrate -Q (µl/min)	Velocity (m/sec)
2.55	1 & 10	10	0.11

The Comsol model can be seen in Fig. 4, which is a simplified model that does not have the relaxing chambers of the PDMS mold.

Model is solved through sequence of geometry creation, boundary condition assignment, parameter entrance and meshing followed by solvers of three studies as electrostatic, laminar – incompressible flow and particle tracing for fluid flow.

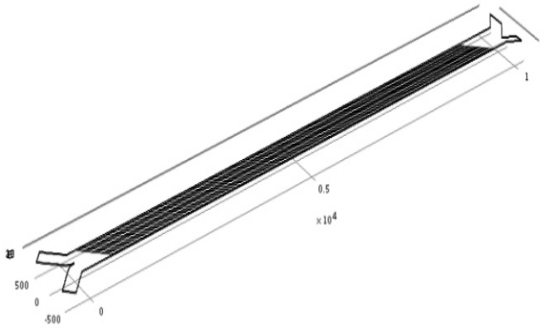

Fig. 4: Comsol model used in the simulations

4. Fabrication and experimental setup

Fabrication of the design performed with photolithography techniques. LOC device consist of glass substrate, titanium electrode coating on glass substrate, PDMS micro channels, electrical and fluidic connections that fabricated with micro-technology. Physical vapor deposition of Titanium, positive (For the electrodes) and negative (For PDMS mold) photoresist processing, plasma bonding (glass to PDMS), PDMS molding for channel and copper wire connection with the conductive epoxy has been performed for fabricating the device (Altinagac et al., 2014).

Fig. 5a shows the fabricated LOC device details which include the copper wirings, microfluidic tubes and connectors and Fig.5b shows the experimental setup.

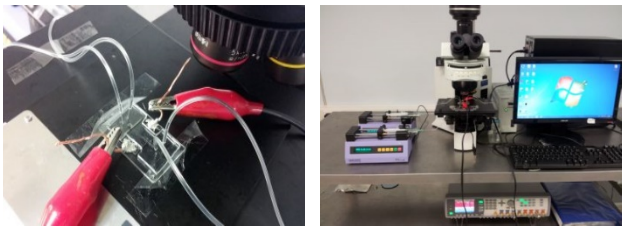

a b

Fig. 5: Experiment details a) fabricated LOC device, b) experimental setup

Experiments has been performed after BSA in PBS solution kept inside the microchannel for 1 day to inhibit fouling (Arun et al., 2011).

5. Results

Electric potentials in the model shown in the Fig. 5 in which there is an applied voltage from -10 V and +10 V load applied to electrode couples. The resulting electric potential distribution along the channel can be seen on Fig. 6. Maximum electric field gradient is around 7x10^5 V m^{-1} and occurs at the edges of the electrodes.

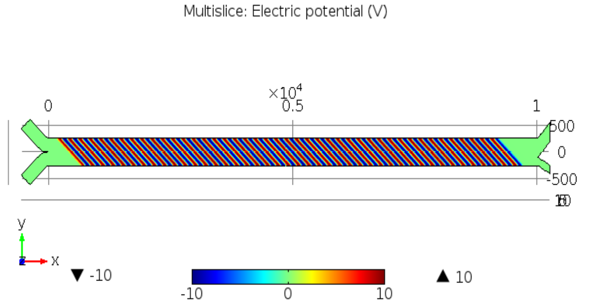

Fig. 6: Electric potential of the model

Velocity field, 0.11 m/s, is applied from the two inlets located in the left side. The friction in micro channels neglected and slip boundary condition applied because of that the velocity is very similar near the channel walls can be seen on Fig. 6, the larger exit velocity is higher and around 0.16 m/s (An analogy can explain better – electric chooses the short circuit).

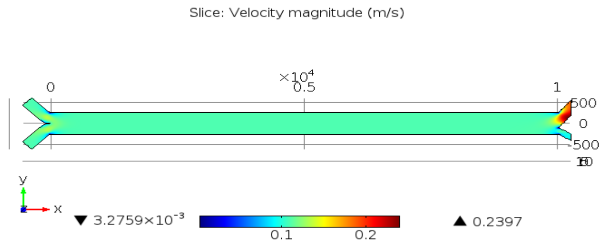

Fig. 6: Velocity profile in the microchannel

The generated electric field and velocity field coupled in to the particles and particle flow for fluid flow study was performed with time dependently and particle trajectories were obtained. In addition, parametric sweep for 3.2 μm (red fluorescent) and 9.8 μm (green fluorescent) implemented in to the study to solve both in one model and it enables to obtain single image of both particles trajectories. Particle trajectories in 1V potential and 10 μl/min (0.11 m/s) (No separation observed, Fig. 7a), and particle trajectories in 10V potential and 10 μl/min (0.11 m/s) (Separation observed, Fig. 7b) is demonstrated.

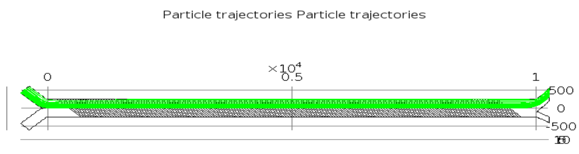

(a)

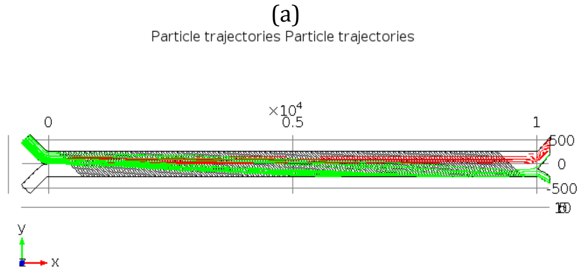

(b)

Fig. 6: Particle trajectories at 1 (a) and 10V (b) potential and 10 μl/min (0.11 m/s)

In order to create a meaningful result separation parameter calculated by using the point average values of all particles. Average of initial position has been subtracted from the final positions and divided by maximum of this position change. Table 2 shows the separation percentages of the model according to the particle diameters and average of particle position in initial and final positions.

Table 2: Results of the model simulations

Flowrate (µl/dk)	Velocity (m/sn)	Potential Vmax (V)	Particle diameter (µm)	Separation percentage	Start position average (µm)	Final position average (µm)	Change in Y axis (µm)
10	0.11	1	3.2	0.111	484	390	94
10	0.11	1	9.8	0.114	484	388	96
10	0.11	10	3.2	0.115	484	387	97
10	0.11	10	9.8	1.000	484	-363	847

Fig. 8 shows the average particle position changes in y direction along the channel and it shows that particles separated from each other.

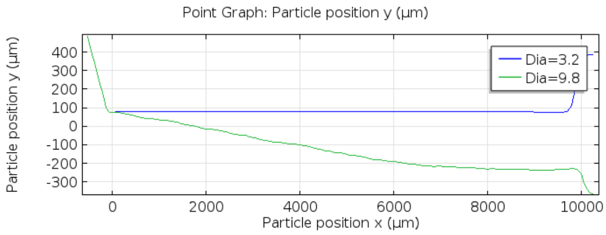

Fig. 8: Average particle position changes in Y-axis

In order to understand the reason behind the separation, DEP force Y component on the Fig. 9 needs to be observed. The effect in 9.8 um particles are much higher and this enables the separation of the larger sized particle.

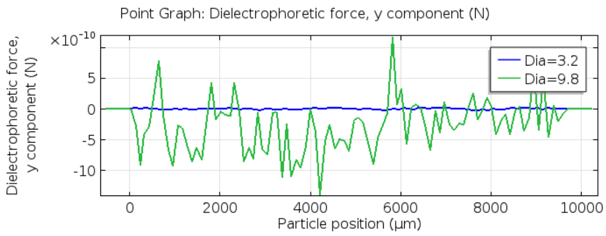

Fig. 9: Average DEP force acting on particles at Y-axis

The inlet and outlets of the channel has been chosen as Region of interest for the experimental observation which can be seen in Fig. 10. The fluorescence images collected from these ROI's and overlaid for 30 sec. to get fluorescence profiles of particle trajectories.

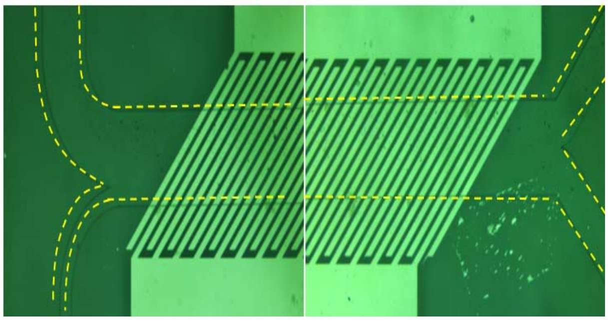

Fig. 10: Region of interest in experimentation (inlet right and outlet left)

Fig. 11 and 12 show that green and red particles are not affected by the negative DEP force at the 1V potential and 10 µl/min flow rate which is in correlation with the experiment.

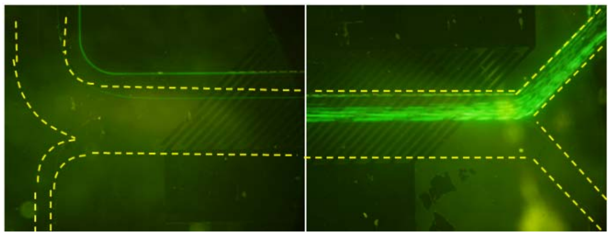

Fig. 11: 1V 10 µl/min results of 9.8 µm particles

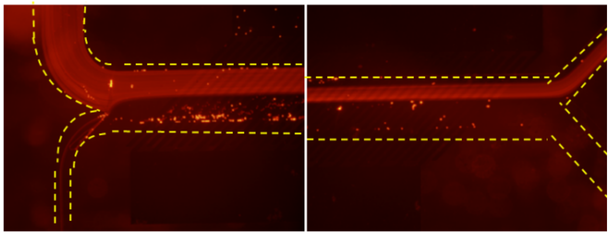

Fig. 12: 1V 10 µl/min results of 3.2µm particles

Figs. 13 and 14 are shown that green particles are affected by the negative DEP force and leaves the channel from the below outlet while the red particles are not affected by the negative DEP force and leaves the channel from the upper outlet.

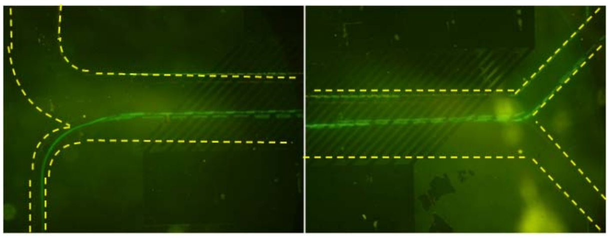

Fig. 13: 10V 10 µl/min results of 9.8 µm particles

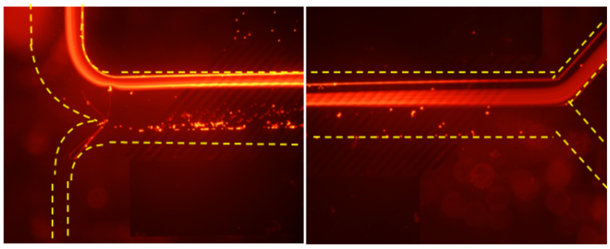

Fig. 14: 10V 10 µl/min results of 3.2 µm particles

6. Conclusion

We studied poystrene particle separation with sizes of 3.2 and 9.8 μm and the simulation results were compared with experiments. It was seen that applied voltage and flow rate were very effective parameters to induce effective DEP force to direct particles effectively. We separated 9.8 μm sized particles from 3.2 μm sized ones in the experiments with a verification of simulation.

Acknowledgment

The authors would like to acknowledge the financial support provided by the Scientific and Technological Research Council of Turkey (TUBITAK) under Grant No. 111M730.

References

Altinagac E, Genc Y, Kizil H, Trabzon L and Beskok A. (2014). Microdevices for continuous sized based sorting by AC dielectrophoresis. In 4th Micro and Nano Flows Conference, UCL, London, UK, 117(4): 1-6.

Altinagac E, Ozcan SS, Genc Y, Kizil H and Trabzon L (2015). Biological particle manipulation: an example of Jurkat enrichment. InNano/Micro Engineered and Molecular Systems (NEMS), 2015 IEEE 10th International Conference on (pp. 25-27). IEEE.

Arun A, Salet P and Ionescu AM (2011). Carbon Nanotube Crossed Junction by Two Step Dielectrophoresis. Journal of Nanoscience and Nanotechnology, 11(6): 4919-4922.

Green NG, Ramos A and Morgan H (2002). Numerical solution of the dielectrophoretic and travelling wave forces for interdigitated electrode arrays using the finite element method. Journal of Electrostatics, 56(2): 235-254.

Khoshmanesh K, Nahavandi S, Baratchi S, Mitchell A and Kalantar-zadeh K (2011). Dielectrophoretic platforms for bio-microfluidic systems. Biosensors and Bioelectronics, 26(5): 1800-1814.

Pethig R. (2010). Dielectrophoresis: status of the theory, technology, and applications. Biomicrofluidics, 4(2): 022811.